Published in final edited form as:
Biomaterials. 2013 April ; 34(13): 3256–3269. doi:10.1016/j.biomaterials.2013.01.028.

The effect of age and emphysematous and fibrotic injury on the re-cellularization of de-cellularized lungs

Dino Sokocevic[a,1,2], **Nicholas R. Bonenfant**[a,1,2], **Darcy E. Wagner**[a,2], **Zachary D. Borg**[a,2], **Melissa J. Lathrop**[a,2], **Ying Wai Lam**[b,3], **Bin Deng**[b,3], **Michael J. DeSarno**[c,4], **Taka Ashikaga**[c,4], **Roberto Loi**[d,5], **Andrew M. Hoffman**[e], and **Daniel J. Weiss**[a,*]

Dino Sokocevic: dino.sokocevic@med.uvm.edu; Nicholas R. Bonenfant: nicholas.bonenfant@med.uvm.edu; Darcy E. Wagner: darcy.wagner@uvm.edu; Zachary D. Borg: zachary.borg@med.uvm.edu; Melissa J. Lathrop: mlathrop@uvm.edu; Ying Wai Lam: ylam@uvm.edu; Bin Deng: bdeng@uvm.edu; Michael J. DeSarno: mdesarno@uvm.edu; Taka Ashikaga: tashikaga@uvm.edu; Roberto Loi: rloi@unica.it; Andrew M. Hoffman: Andrew.Hoffman@tufts.edu; Daniel J. Weiss: dweiss@uvm.edu

[a]Department of Medicine, University of Vermont College of Medicine, 226 Health Science Research Facility, Burlington, VT 05405, United States

[b]Department of Biology, University of Vermont College of Arts and Sciences, 311 Marsh Life Sciences, Burlington, VT 05405, United States

[c]Biostatistics Unit, University of Vermont College of Medicine, 27 Hills Building, Burlington, VT 05405, United States

[d]Department of Biomedical Sciences, University of Cagliari, Italy

[e]Department of Clinical Sciences, Tufts University, Cummings School of Veterinary Medicine, Bldg 21, Suite 102, 200 Westboro Road, North Grafton, MA 01536, United States

Abstract

Use of de-cellularized cadaveric lungs as 3-dimensional scaffolds for *ex vivo* lung tissue generation offers a new potential therapeutic approach for clinical lung transplantation. However, it is likely that some of the available cadaveric human lungs may be from older donors or from donors with previously existing structural lung diseases such as emphysema or pulmonary fibrosis. It is not known whether these lungs will be suitable for either de-cellularization or re-cellularization. To investigate this, we assessed the effects of advanced age, representative emphysematous and fibrotic injuries, and the combination of advanced age and emphysematous injury and found significant differences both in histologic appearance and in the retention of extracellular matrix (ECM) and other proteins, as assessed by immunohistochemistry and mass

[*]Corresponding author. Tel.: +1 802 656 8925; fax: +1 802 656 8926.
[1]Contributed equally to this work.
[2]Tel.: +1 802 656 8110; fax: +1 802 656 8926.
[3]Tel.: +1 802 656 9722; fax: +1 802 656 2914.
[4]Tel.: +1 802 656 2526; fax: +1 802 656 3632.
[5]Tel.: +39 070 675 8638; fax: +39 070 666 062

Appendix A. Supplementary data

Supplementary data related to this article can be found at http://dx.doi.org/10.1016/j.biomaterials.2013.01.028.

Disclosure statement

No competing financial interests exist.

spectrometry, between the different conditions. However, despite these differences, binding, retention and growth of bone marrow-derived mesenchymal stromal cells (MSCs) over a 1-month period following intratracheal inoculation were similar between the different experimental conditions. In contrast, significant differences occurred in the growth of C10 mouse lung epithelial cells between the different conditions. Therefore, age, lung injury, and the cell type used for re-cellularization may significantly impact the usefulness of de-cellularized whole lungs for *ex vivo* lung tissue regeneration.

Keywords

Acellular matrix; Age; Epithelial cell; Extracellular matrix (ECM); Lung; Mesenchymal stem cell

1. Introduction

Approximately 1000–1500 lung transplants per year are performed in the United States, but a significant shortage of suitable donor lungs and the drawbacks of lung transplantation, including lifelong immunosuppression and an approximate 50% 5-year mortality, demonstrate a critical need for new approaches [1]. Although transplantation of cadaveric lungs has not yet been feasible to date, use of de-cellularized whole lung as scaffolds for *ex vivo* lung bioengineering has recently been investigated as an alternative approach that could potentially allow use of cadaveric lungs seeded with autologous stem or progenitor cells obtained from the eventual transplant recipient [2-13].

However, some of the donor lungs that might be utilized for de-cellularization and *ex vivo* bioengineering may originate from aged donors, donors with pre-existing structural lung diseases, or a combination of both age and lung disease. At present it is unknown how these factors might affect either de-cellularization or subsequent re-cellularization. To assess these questions, we comparatively assessed architecture and ECM content in de-cellularized mouse lungs from young (8–12 weeks) vs. old (15–18 months) mice, lungs from young mice after induction of either emphysematous lung injury following intratracheal inoculation with elastase or of fibrotic injury following intratracheal instillation of bleomycin, or in young mice injured with elastase and allowed to age. We then further assessed growth of two different cell types, murine bone marrow-derived mesenchymal stromal cells (MSCs) and C10 mouse lung epithelial cells following intratracheal inoculation into the different de-cellularized lungs.

2. Materials and methods

2.1. Mice

Adult C57BL/6J male mice aged 8–12 weeks (young mice) or 15–18 months (old mice) (Jackson Laboratories), were maintained at UVM in accordance with institutional and American Association for Accreditation of Laboratory Animal Care (AAALAC) standards and review.

2.2. Lung de-cellularization

Mice were euthanized by lethal intraperitoneal injection of sodium pentobarbital in accordance with accepted AAALAC standards. After opening the chest, the trachea was cannulated with a blunted 18 gauge Luer-lock syringe. The thymus was removed and discarded and the heart–lung bloc was harvested. The lungs were de-cellularized under sterile conditions as follows [3,8,9,11]. Each step listed was accomplished by both rinsing through the trachea, and by perfusing solutions through the right ventricle. Lungs were washed in a 5× penicillin/streptomycin solution (from 100× stock, Cellgro) in de-ionized water (DI), for 1 h at 4 °C. Three cc of DI were injected through the cannulated trachea to rinse the lung, which was allowed to deflate before repeating the tracheal rinse another four additional times. A DI rinse of 15 cc was repeated through the vasculature by injection through the right ventricle. Next, 3 cc of 0.1% Triton-X (Sigma) and 5× pen/strep in DI were infused through both the trachea and the right ventricle. The lungs were submerged in Triton-X solution and incubated at 4 °C for 24 h. The following day, the lungs were removed from the Triton solution and rinsed with DI/pen-strep as described above. Three cc of 2% sodium deoxycholate (Sigma) and 1× pen/strep in DI water were then infused through the trachea and right ventricle and the lungs incubated in this solution at 4 °C for 24 h. The lungs were then removed from the sodium deoxycholate solution and rinsed with DI as described above. Three cc of 1 M NaCl (USB, Cleveland, OH) and 5× pen/strep were then infused through the trachea and right ventricle. The lungs were incubated in this solution for 1 h at room temperature (~25 °C). The lungs were removed from the NaCl solution and rinsed with DI water as described above. Three cc of 30 μg/mL porcine pancreatic DNase (Sigma), 1.3 mM MgSO4 (Sigma), 2 mM CaCl2 (Sigma), 5× pen/strep in DI water were infused through the trachea and right ventricle, and the lungs incubated in this solution for 1 h at room temperature. Finally the lungs were removed from the DNase solution and rinsed with 5× pen/strep in 1× PBS as described above for the DI solution rinses. Lungs were stored in PBS/pen-strep solution at 4 °C until utilized [3,8,9].

2.3. Lung injury

To induce emphysematous lung injury in mice, porcine pancreatic elastase (USB, Cleveland, OH) was instilled by oropharyngeal inoculation at a dose of 135 IU/mg (1.5 IU PPE) per kg body weight (Elastin Products, St Louis, MO) [14]. Mice were euthanized either 1 month later (young mice) or approximately 43–68 weeks later (old mice) and the heart–lung blocs subsequently de-cellularized. To induce fibrotic lung injury in mice, 0.075 U/mouse of bleomycin (APP Pharmaceutical, Schaumburg, IL) was instilled by oropharyngeal inoculation [15]. The heart–lung blocs were harvested 14 days post-instillation and subsequently de-cellularized.

2.4. Lung histology

De-cellularized lungs were fixed (20 cm H_2O) with 4% paraformaldehyde for 10 min at room temperature, and embedded in paraffin. 5 μm sections were cut and mounted on glass slides. Following deparaffinization, sections were stained with hematoxylin & eosin (H&E), Verhoeff's Van Gieson (EVG), Masson's Trichrome, or Alcian Blue, and were assessed by standard light microscopy [8,9].

2.5. Immunohistochemical (IHC) staining

Standard deparaffinization was performed with three 10 min xylene incubations followed by rehydration in descending ethanol series and water. Antigen retrieval was performed in 10 mM sodium citrate buffer (Dako, Carpentaria, CA) at 98 °C for 20 min. Tissue sections were then allowed to cool down at room temperature for 20 min. Tissue sections were permeabilized with a 0.1% Triton-X solution (Sigma Aldrich, St. Louis, MO) for 15 min. Triton-X was removed with two 10 min washes in 1% BSA solution. Blocking was performed with 10% goat serum for 1 h at room temperature. After blocking, primary antibodies were added in their appropriate concentrations. Primary antibodies used were: Purified Mouse Anti-Fibronectin monoclonal (610077 Fibronectin – 1:100, BD Transduction Laboratories), Laminin antibody polyclonal (ab11575 – 1:100, Abcam), Smooth muscle myosin heavy chain 2 polyclonal (ab53219 – 1:100, Abcam), Collagen I polyclonal (ab292 – 1:100, Abcam), Rabbit polyclonal to alpha elastin (ab21607 – 1:100, Abcam), Ki67 Proliferation marker polyclonal (ab16667 – 1:50, Abcam), Cleaved Caspase-3 polyclonal (Asp175 – 1:100, Cell Signaling Technology), Mouse clone anti-human Actin polyclonal (1A4 – 1:10,000, Dako). Tissue sections were incubated overnight at 4 °C in a humidified chamber with the primary antibody. The tissue slides were then washed three times with 1% BSA solution for 5 min each. A proper secondary antibody was added and sections were incubated for 1 h at room temperature in a humidified dark chamber. Two secondary antibodies were used; Alexa Fluor 568 goat anti-rabbit IgG (H + L) (1:500, Invitrogen, Grand Isle, NY), and Alexa Fluor 568 $F(ab')_2$ fragment of goat anti-mouse IgG (H + L) (1:500, Invitrogen, Grand Isle, NY). After the 1 h incubation, the tissue was washed three times in 1% BSA solution for 5 min each in the dark. A DAPI nuclear stain was added for 5 min at room temperature in the dark, and was followed by 2 washes in 1% BSA solution for 5 min each. Tissue sections were then mounted in Aqua Polymount (Lerner Laboratories, Pittsburg, PA).

2.6. Mass spectrometry

Samples (approximately 1 cm^3 and 130 mg for each sample) obtained from the right lower lobe of the various lungs were processed according to standard protocol [8,9] and dried separately in a SpeedVac. Each dried sample was then suspended in 40 μL of 100 mM ammonium bicarbonate (NH_4HCO_3)/50 mM dithiothreitol and placed at 56 °C for 1 h. After cooling, 5 μL of 500 mM iodoacetamide in 100 mM NH_4HCO_3 was added, and the solution was incubated for 30 min at room temperature in the dark. The sample was then dried in a SpeedVac, suspended in 50 μL of trypsin solution (10 ng/mL) in 50 mM NH_4HCO_3, and incubated overnight at 37 °C. Five microliters of 10% formic acid was then added to stop the digestion. The sample was then centrifuged at 14,000*g*, and 15 μL of supernatant was desalted using a C18 ZipTip (P10; Millipore Corporation) according to the manufacturer's protocol. The ZipTip eluate was then dried again, and then reconstituted in 20 μL 0.1% formic acid and 2% acetonitrile. Six microliters of each digest was loaded directly onto a 100 μm × 120 mm fused silica microcapillary column packed with MAGIC C18 (5 μm particle size, 20 nm pore size, Michrom Bioresources) at a flow rate of 500 nL/min, and peptides were separated by a gradient comprising 3–60% ACN/0.1% formic acid in 45 min. The peptides were introduced into a linear ion trap (LTQ)-Orbitrap mass spectrometer (Thermo Fisher Scientific) via a nanospray ionization source. Mass spectrometry data was

acquired in a data-dependent acquisition mode, in which an Orbitrap survey scan from *m*/*z* 400–2000 (resolution: 30,000 FWHM at *m*/*z* 400) was paralleled by 10 LTQ MS/MS scans of the most abundant ions.

The product ion spectra were searched against the IPI mouse database (v. 3.75) using SEQUEST (Bioworks 3.3.1, Thermo Fisher Scientific). Search parameters allowed mass tolerances of 2.0 Da and 1.4 Da for precursor and fragment ions, respectively, and variable modifications for oxidized methionine (+15.9949 amu) and carboxyamidomethylated cysteine (+57.021464 amu). After applying filters of cross correlation XCorr [1.9, 2.5, 3.8 for peptide charge states of +1, +2, and +3, respectively], delta correlation (ΔCN) (>0.1) and peptide probability (<1e-3), protein identifications were ranked by number of peptides identified. Proteins that were identified by two or more peptides in each of the replicates were compiled and the average number of peptides identified from multiple replicates for each protein was presented in Supplementary Table 1.

2.7. Cells and cell inoculation

Mesenchymal stromal cells (MSCs) derived from bone marrow of adult male C57BL/6 mice were obtained from the NCRR/NIH Center for Preparation and Distribution of Adult Stem Cells at Texas A andMUniversity [16]. Purity was established at Texas A and M University by expression of Sca-1, CD106, CD29, CD45, absence of CD11b, CD11c, CD34, and the ability to differentiate into osteoblasts, chondrocytes and adipocytes *in vitro* [16]. C10 mouse lung epithelial cells were obtained courtesy of Matthew Poynter PhD, University of Vermont and cultured under standard conditions [17]. The MSCs were cultured on cell-culture treated plastic at 37 °C and 5% CO_2 in MSC basal medium consisting of Iscove's Modification of Dulbecco's Medium supplemented with 2 m_{ML}-glutamine, 100 U/mL penicillin and 100 μg/mL streptomycin (Fisher), 10% fetal bovine serum (Atlanta Biologicals) and 10% horse serum (HS, Invitrogen). Cells were used at passage 9 (or lower), and were maintained in culture at confluency no greater than 70%.

To seed the de-cellularized lungs, a solution of 3% low-melting temperature SeaPrep Agarose (Cambrex) in PBS was warmed until the agarose melted. $1 \times 10_6$ MSCs or C10 cells suspended in 1 mL MSC or C10 basal media, respectively, were mixed with 1 mL of the low-melting agarose and the 2 mL cell suspension injected through the cannulated trachea. Only the left lobe of the de-cellularized lungs was used for seeding. To ensure this, the right lobes were tied off using sterile suture under sterile conditions, and the right lobes were then removed. The inoculated lung was then incubated for 30 min at 4 °C until the agarose hardened and the lobe sliced with a sterile razor blade to yield transverse sections of an approximately 1 mm thickness. Each slice was placed in a well of a 24 well dish, covered with sterile cell media, and placed in a standard tissue culture incubator at 37 °C until the agarose melted out of the tissue [9]. The lungs were submerged overnight in basal MSC or C10 media at 37 °C and 5% CO_2. The next day, medium was changed to fresh basal medium and then changed every other day. Individual slices were harvested at 1, 3, 7, 14, 21, and 28 days post-inoculation, and were fixed for 10 min at room temperature in 4% paraformaldehyde. Samples were embedded in paraffin, then were cut and mounted as 5 μm

paraffin sections. These sections were assessed by H&E staining for presence and distribution of the inoculated cells.

3. Statistical analyses

Heat maps for the natural log of unique peptide hits for each positively identified protein in the mass spectrometric analyses of lungs de-cellularized under each experimental condition were generated using the 'pheatmap' package for 'R' statistical software version 2.15.1. Two group comparisons were done using the raw peptide counts (i.e. non-log transformed) using the non-parametric exact permutation test with $p < 0.05$ considered statistically significant [18]. This non-parametric equivalent of the *t*-test was used due to the non-normality of the data, small sample sizes per group, and to directly compare biologically relevant conditions. As a measure of agreement/concordance between lung lobe sample replicates, non-parametric Spearman correlations were also done with concordance considered significant at $p < 0.05$ [18]. The exact permutation tests and correlations were done using SAS statistical software, version 9.2.

4. Results

4.1. Comparison of de-cellularized lungs obtained from young, old, elastase, and bleomycin-treated mice

As we and others have previously demonstrated, architecture is largely preserved in de-cellularized lungs obtained from young healthy mice, as assessed by H&E, Masson's Trichrome (collagen), and Von Gieson's (elastin) staining (Fig. 1A, [3-12]). There is an overall decrease in Alcian Blue staining for glycosaminoglycans (GAGS, Fig. 1A and B panels G, H, I, likely reflecting loss of cell associated GAGs [3-12]). In contrast, age-related degenerative changes, including mixed emphysematous and fibrotic-appearing architecture were observed in de-cellularized lungs obtained from aged mice (Fig.1A, Supplemental Fig. 1). Instillation of elastase into young mice resulted in marked emphysematous changes in native lungs, changes that were preserved in the de-cellularized lungs obtained from mice 4 weeks after elastase instillation (Fig. 1B, Supplemental Fig. 1). If elastase-treated mice were allowed to age, the emphysematous changes were maintained both in native lungs and in the de-cellularized lungs (Fig. 1B, Supplemental Fig. 1). Similarly, mice treated with bleomycin characteristically developed patchy areas of fibrosis in native lungs, changes that were also preserved in de-cellularized lungs (Fig. 1B, Supplemental Fig. 1). Collagen and elastin staining of the de-cellularized lungs reflected the pathologic changes produced by either age or specific injury, changes that were preserved in the de-cellularized lungs. Qualitative assessment of GAGs following de-cellularization was comparable between experimental conditions.

4.2. Comparative immunohistochemical characterization of ECM proteins in the de-cellularized lungs

As previously shown [2-6,8-11], specific immunohistochemical staining for selected ECM proteins demonstrated that type 1 collagen and laminin were largely retained in de-cellularized lungs from young mice whereas elastin was significantly decreased (Fig. 2A, panels J, K, L; Supplemental Fig. 2, panels M, N, O, P). Fibronectin was largely retained but

displayed a fragmented appearance (Fig. 2A and B, panels A, B, C) [8,9]. Some cellular proteins, including smooth muscle actin and smooth muscle myosin, were also retained in patterns similar to those seen in native lungs (Fig. 2A, Supplemental Fig. 2, [8,9]). While the patterns of each specific injury or age condition were retained on immunohistochemical staining, similar to observations with histochemical staining (Fig.1, Supplemental Fig. 1) retention of ECM proteins (type 1 collagen, laminin, fibronectin) as well as smooth muscle actin and smooth muscle myosin was qualitatively comparable between groups (Fig. 2A and B).

4.3. Residual protein content and composition in the de-cellularized Lungs

We hypothesized that residual protein content as determined by mass spectrometry would differ between young and old mice, and normal (young or old) vs. injured lungs. Lungs (right lower lobes) which had been freshly de-cellularized from young naive mice were utilized as controls. Comparisons included old vs. young naive mice, old elastase vs. young elastase-injured mice, old vs. old elastase-injured mice, and young naive mice vs. young bleomycin-injured mice. All IPI accession numbers were manually searched in the UniProtKB/Swiss Prot database (http://www.uniprot.org/help/about). If a protein was matched to more than one category, its predominant subcellular locationwas used for functional grouping. Protein identification was assigned based on two or more unique peptide hits within the same sample, not across samples. A full listing of proteins which were detected above threshold (two or more unique peptide hits) is presented in Supplemental Table 1. Corresponding heat maps (Fig. 3) were generated with proteins broadly categorized as cytoskeletal, extracellular matrix (ECM), intracellular cytoplasmic, intranuclear and membrane proteins. Values presented are log normal transformations of unique peptide hits for each protein in each experimental sample. The majority of statistically significant differences appeared between groups in the ECM proteins (Table 1). As compared to controls, de-cellularized lungs from old mice, or either young or old elastase-treated mice, contained statistically fewer overall ECM proteins. There was no specific pattern in the differences between any of these experimental groups as compared to young controls. In contrast, decellularized lungs from bleomycin-injured mice contained significantly more residual ECM proteins overall, with notable increases in residual collagen 6a, fibrillin, fibrinogen, and fibronectin. De-cellularized lungs from young elastase-treated mice contained more residual overall ECM proteins compared to those from old elastase-treated mice. Similarly there were greater overall residual ECM proteins in de-cellularized lungs from old vs. old elastasetreated mice. While there were statistically significant differences in levels of residual proteins in the other categories (cytoskeletal, cytosolic, membrane, nuclear) between the experimental groups (Table 1, Fig. 3), there was no clear or obvious association between experimental group and residual protein content.

4.4. Growth of MSCs and C10 cells in aged and injured decellularized lungs

On day 1, both MSCs and C10s were observed to primarily engraft in alveolar spaces although some localization around airways and blood vessels was noted at later time points (Figs. 4 and 5). The only noticeable exception was a lower density of cells in the highly fibrotic regions of the bleomycin-injured decellularized lungs compared to less affected

regions, suggesting that the inoculated cells were unable to penetrate into or adhere in these regions following intratracheal inoculation (Figs. 4 and 5, panels I, J).

After 1 day of culture, MSCs acquired a characteristic spindleshaped phenotype, and could similarly be found scattered throughout the different de-cellularized lungs, except the more dense fibrotic regions of the de-cellularized lungs obtained from bleomycin-injured lungs, through 28 days of culture. In contrast, while C10 cells could be found growing throughout the 28-day period in de-cellularized lungs obtained from young, old, and bleomycin-injured mice, except for the denser fibrotic regions in bleomycin lungs, no viable cells were observed past 14 days in lungs obtained from either young or old elastase-injured mice (Fig. 5, panels F, H). Under all conditions, the location of the surviving C10 cells became more peripheral or along larger airways with increased time in culture except for the elastase-injured lungs, in which the cells remain relatively dispersed.

To determine whether the C10s and MSCs were either proliferating and/or undergoing apoptosis during the culture period, Ki67 and caspase-3 staining were done after 1 day of culture and at the last time point at which viable cells were observed for each condition (Figs. 6 and 7). We had previously observed robust Ki67 staining and minimal caspase-3 staining of MSCs at both 1 and 28 days when inoculated into de-cellularized lungs obtained from young healthy mice [8,9]. In the current study, robust Ki67 expression and minimal caspase-3 expression were observed in MSCs after 1 day of culture under each condition (Fig. 6). Following 28 days in culture, less evident Ki67 expression but increased caspase-3 expression was observed, particularly in de-cellularized lungs obtained from elastase or bleomycin-injured lungs.

We had similarly previously observed robust Ki67 and minimal caspase-3 staining following either 1 or 28 days in culture of C10 cells intratracheally inoculated into de-cellularized lungs obtained from young healthy mice [9]. In contrast, less evident Ki67 staining and increased caspase-3 staining were observed at or before the last time point in which viable cells were found for each condition (Fig. 7).

5. Discussion

Lung transplantation is currently limited by a shortage of available donor lungs and by immune reactions to the transplanted lungs resulting in both acute and chronic rejection with significant morbidity and mortality. To date, use of cadaveric lungs has not been feasible. However, use of de-cellularized whole lung scaffolds may provide a viable option for clinical lung transplantation [2-14]. As demonstrated by us and others, de-cellularization to remove cellular materials, and presumably the majority of immune epitopes that may provoke rejection in the transplant recipients, produces a remaining 3-dimensional scaffold that preserves much of the native architecture of the lung. Several approaches have been utilized to produce de-cellularized scaffolds and, although the optimal de-cellularization method has not yet been clearly established, these scaffolds can support re-cellularization with a variety of cell types and also support short term implantation of recellularized lungs.

However, some cadaveric lungs, or even potential live donor lungs that were considered through organ procurement programs but found unsuitable for transplantation, may come

from aged donors or from donors with previously existing structural lung diseases such as emphysema or pulmonary fibrosis. While advanced age or severe cases of either type of disease would not be suitable for consideration, mild or moderately affected lungs could conceivably be utilized for de-cellularization and subsequent recellularization and clinical use. To evaluate this possibility, we assessed de-cellularization and initial re-cellularization of lungs obtained from aged mice and from mice with experimentallyinduced emphysematous or fibrotic lung injury. Notably, the detergent-based de-cellularization approach utilized achieved appropriate de-cellularization with each age and injury condition yet preserved the specific characteristic anatomical injury patterns for each type of injury. The remaining ECM scaffolds for each condition were consistent with the underlying injury and also showed preservation of the characteristic injury patterns, as reflected by both histologic architecture and by proteomic assessment using mass spectrometry. This demonstrates that successful de-cellularization can be achieved in aged and injured lungs and that the resulting lung will reflect the original disease state. These findings are consistent with recent description of de-cellularized cadaveric lungs obtained from patients with idiopathic pulmonary fibrosis [19].

The use of mass spectrometry to assess residual proteins remaining in de-cellularized lung scaffolds is useful as a high throughput screening approach as the range of proteins detected is far more accessible than that obtained with histologic or immunohistologic (IHC) assessments. A range of minor proteins remaining in the scaffold that make up the complex ECM scaffold that would not normally be probed by IHC or western analyses can be detected [8-10,20]. This could provide critical information on whether necessary proteins remain and also whether undesirable proteins, ECM or otherwise, may remain and is useful as a tool for comparing different de-cellularization approaches. However, the sensitivity and specificity of mass spectrometry may be less than that afforded by IHC or western analyses using highly specific monoclonal antibodies directed toward relevant epitopes critical for binding and or growth and differentiation of inoculated cells. As such, biologically relevant information provided by mass spectrometry may be limited and more relevant information is provided by the behavior of cells inoculated into the different origin decellularized lungs.

Initial binding and subsequent survival and proliferation of a stromal cell line (MSCs) inoculated into the airways were robust across the different conditions and comparable to that observed following inoculation into de-cellularized lungs obtained from young healthy mice. The only exception was lack of initial cell engraftment and subsequent growth in the more densely fibrotic regions of the bleomycin-injured lungs. This suggests that, despite changes resulting from age and/or injury, appropriate preservation of the ECM structures necessary for initial binding and subsequent growth and proliferation were generally preserved. Similarly, initial engraftment and subsequent viability of an immortalized type 2 alveolar epithelial cell line (C10) were similar in aged and bleomycin-injured lungs compared to that observed following inoculation of C10 cells into freshly de-cellularized normal lungs [9]. Comparable recent data suggests that fibroblasts cultured *in vitro* on scaffolds consisting of pieces of de-cellularized lungs obtained from patients with idiopathic pulmonary fibrosis will survive, proliferate, and are also induced to acquire a myofibroblast phenotype [19].

In contrast, despite good initial engraftment, survival of the C10 cells was diminished in emphysematous lungs produced by elastase treatment in both young and old mice. The reasons for this are not yet clear but one conceivable explanation is that, despite gross preservation of ECM proteins in the elastase-injured lungs, more subtle changes in the ECM scaffold do not support longer term proliferation and survival of the C10 cells. Of note, there was minimal elastin remaining in young naive de-cellularized lungs and thus no significant differences were detected between those compared to either young or old elastase-injured de-cellularized lungs.

6. Conclusion

These results suggest that de-cellularized lungs obtained from aged lungs may be appropriate for *ex vivo* lung bioengineering approaches utilizing de-cellularization and re-cellularization strategies. However, a wider range of cell types, including pulmonary vascular endothelial cells and different stem and progenitor cell populations that might be utilized for re-cellularization, need to be tested. Our data suggests that fibrotic lungs support prolonged growth of inoculated cells but whether these lungs will be useful for long-term regeneration is unclear. This suggests that the specific scaffold obtained from de-cellularization of lungs from different disease states can significantly affect cell growth and differentiation. Accordingly, we found that de-cellularized emphysematous lungs may not support long-term viability of epithelial cells. Careful and rigorous attention needs to be given to better understand all of the conditions that will affect lung procurement, de-cellularization, re-cellularization, immunogenicity, and eventual clinical implantation. Further exploration of the potential use of aged and diseased lungs will yield continuing insight into both the potential clinical usefulness of these lungs and the mechanisms by which the residual ECM scaffold can influence growth and differentiation of inoculated cells.

Supplementary Material

Refer to Web version on PubMed Central for supplementary material.

Acknowledgments

The authors gratefully acknowledge the staffs of the Offices of Animal Care Management at the University of Vermont, Bruce Bunnell and Christine Finck for critical reads of the manuscript and Tyler Bittner and Ian Johnson for valuable contributions to the experimental studies. Studies were supported by NIH ARRA RC4HL106625 (D.J.W.), NHLBI R21HL094611 (D.J.W.), UVM Lung Biology Training grant T32 HL076122 from the NHLBI, and UVM Environmental Pathology Training grant T32 ES007122 from the NIEHS. Facilities and equipment were supported by the UVM Lung Biology COBRE (NIH NCRR P20 RR-155557), the Vermont Cancer Center DNA Analysis facility (NIH P30 CA22435), and the Vermont Genetics Network through Grant Number 8P20GM103449 from the INBRE Program of the National Institute of General Medical Sciences (NIGMS) and the National Center for Research Resources (NCRR).

References

1. Orens JB, Garrity ER Jr. General overview of lung transplantation and review of organ allocation. Proc Am Thorac Soc. 2009; 6:13–9. [PubMed: 19131526]
2. Panoskaltsis-Mortari A, Weiss DJ. Breathing new life into lung transplantation therapy. Mol Ther. 2010; 18:1581–3. [PubMed: 20808323]

3. Price AP, England KA, Matson AM, Blazar BR, Panoskaltsis-Mortari A. Development of a decellularized lung bioreactor system for bioengineering the lung: the matrix reloaded. Tissue Eng Part A. 2010; 16:2581–91. [PubMed: 20297903]
4. Cortiella J, Niles J, Cantu A, Brettler A, Pham A, Vargas G, et al. Influence of acellular natural lung matrix on murine embryonic stem cell differentiation and tissue formation. Tissue Eng Part A. 2010; 16:2565–80. [PubMed: 20408765]
5. Petersen TH, Calle EA, Zhao L, Lee EJ, Gui L, Raredon MB, et al. Tissue-engineered lungs for in vivo implantation. Science. 2010; 329:538–41. [PubMed: 20576850]
6. Ott HC, Clippinger B, Conrad C, Schuetz C, Pomerantseva I, Ikonomou L, et al. Regeneration and orthotopic transplantation of a bioartificial lung. Nat Med. 2010; 16:927–33. [PubMed: 20628374]
7. Song JJ, Kim SS, Liu Z, Madsen JC, Mathisen DJ, Vacanti JP, et al. Enhanced in vivo function of bioartificial lungs in rats. Ann Thorac Surg. 2011; 92:998–1005. discussion 6. [PubMed: 21871290]
8. Daly AB, Wallis JM, Borg ZD, Bonvillain RW, Deng B, Ballif BA, et al. Initial binding and recellularization of decellularized mouse lung scaffolds with bone marrow-derived mesenchymal stromal cells. Tissue Eng Part A. 2012; 18:1–16. [PubMed: 21756220]
9. Wallis JM, Borg ZD, Daly AB, Deng B, Ballif BA, Allen GB, et al. Comparative assessment of detergent-based protocols for mouse lung de-cellularization and re-cellularization. Tissue Eng Part C Methods. 2012; 18:420–32. [PubMed: 22165818]
10. Jensen T, Roszell B, Zang F, Girard E, Matson A, Thrall R, et al. A rapid lung decellularization protocol supports embryonic stem cell differentiation in vitro and following implantation. Tissue Eng Part C Methods. 2012; 18:632–46. [PubMed: 22404373]
11. Bonvillain RW, Danchuk S, Sullivan DE, Betancourt AM, Semon JA, Eagle ME, et al. A nonhuman primate model of lung regeneration: detergent-mediated decellularization and initial in vitro recellularization with mesenchymal stem cells. Tissue Eng Part A. 2012; 18:2437–52. [PubMed: 22764775]
12. Petersen TH, Calle EA, Colehour MB, Niklason LE. Matrix composition and mechanics of decellularized lung scaffolds. Cells Tissues Organs. 2012; 195:222–31. [PubMed: 21502745]
13. Badylak SF, Weiss DJ, Caplan A, Macchiarini P. Engineered whole organs and complex tissues. Lancet. 2012; 379:943–52. [PubMed: 22405797]
14. Hoffman AM, Paxson JA, Mazan MR, Davis AM, Tyagi S, Murthy S, et al. Lung-derived mesenchymal stromal cell post-transplantation survival, persistence, paracrine expression, and repair of elastase-injured lung. Stem Cells Dev. 2011; 20(10):1779–92. [PubMed: 21585237]
15. Ortiz LA, Gambelli F, McBride C, Gaupp D, Baddoo M, Kaminski N, et al. Mesenchymal stem cell engraftment in lung is enhanced in response to bleomycin exposure and ameliorates its fibrotic effects. Proc Natl Acad Sci U S A. 2003; 100(14):8407–11. [PubMed: 12815096]
16. Sekiya I, Larson BL, Smith JR, Pochampally R, Cui JG, Prockop DJ. Expansion of human adult stem cells from bone marrow stroma: conditions that maximize the yields of early progenitors and evaluate their quality. Stem Cells. 2002; 20:530–41. [PubMed: 12456961]
17. Malkinson AM, Dwyer-Nield LD, Rice PL, Dinsdale D. Mouse lung epithelial cell lines e tools for the study of differentiation and the neoplastic phenotype. Toxicology. 1997; 123:53–100. [PubMed: 9347924]
18. Zar, JH. Biostatistical analysis. Englewood Cliffs, N.J.: Prentice-Hall; 1974.
19. Booth AJ, Hadley R, Cornett AM, Dreffs AA, Matthes SA, Tsui JL, et al. Acellular normal and fibrotic human lung matrices as a culture system for in vitro investigation. Am J Respir Crit Care Med. 2012; 186(9):866–76. [PubMed: 22936357]
20. Welham NV, Chang Z, Smith LM, Frey BL. Proteomic analysis of a decellularized human vocal fold mucosa scaffold using 2D electrophoresis and high-resolution mass spectrometry. Biomaterials. 2013; 34:669–76. [PubMed: 23102991]

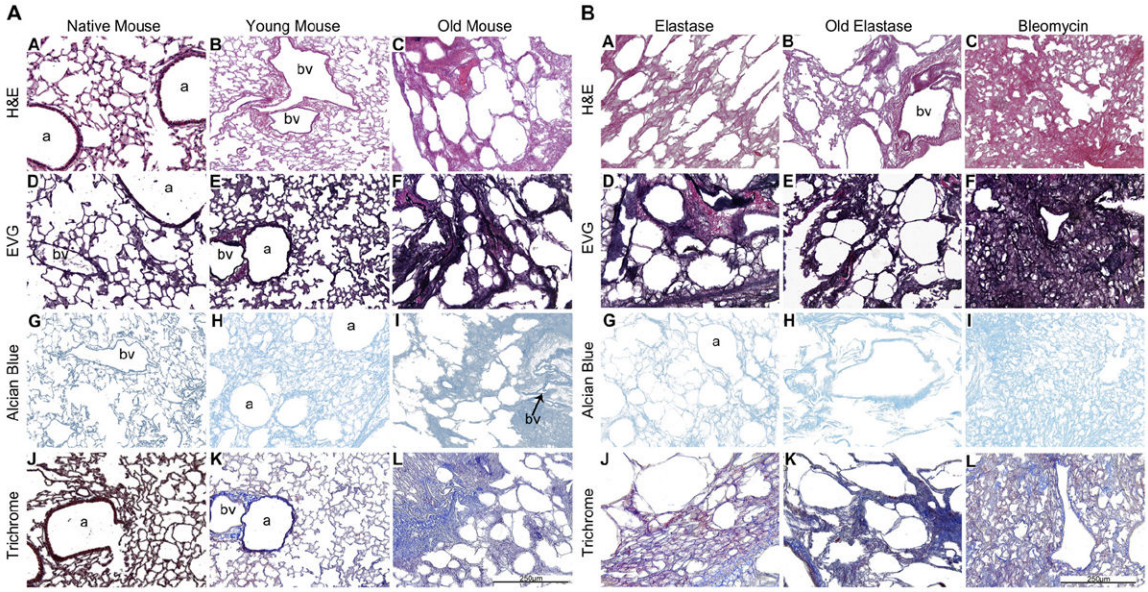

Fig. 1.

A: The de-cellularization process preserves the mouse lung architecture. Representative photomicrographs show native young mouse lungs and de-cellularized lungs obtained from both young and old mice. *N* = 6 for each condition. a = airways, bv = blood vessels. Original magnification 200×. **B: Elastase and bleomycin alter the architecture of the mouse lung scaffold**. Representative photomicrographs demonstrate the effects of elastase in both young and old mice and of bleomycin in young mice on architecture of the de-cellularized lungs. *N* = 6 for each condition. a = airspaces, bv = blood vessels. Original magnification 200×.

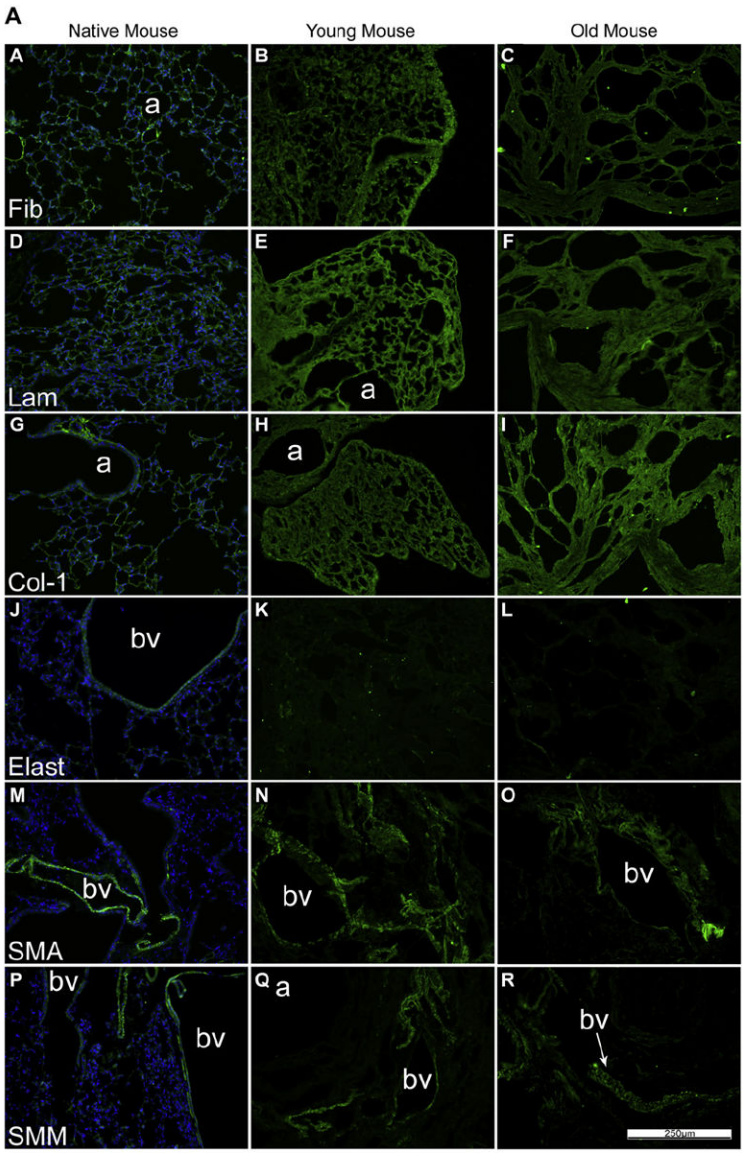

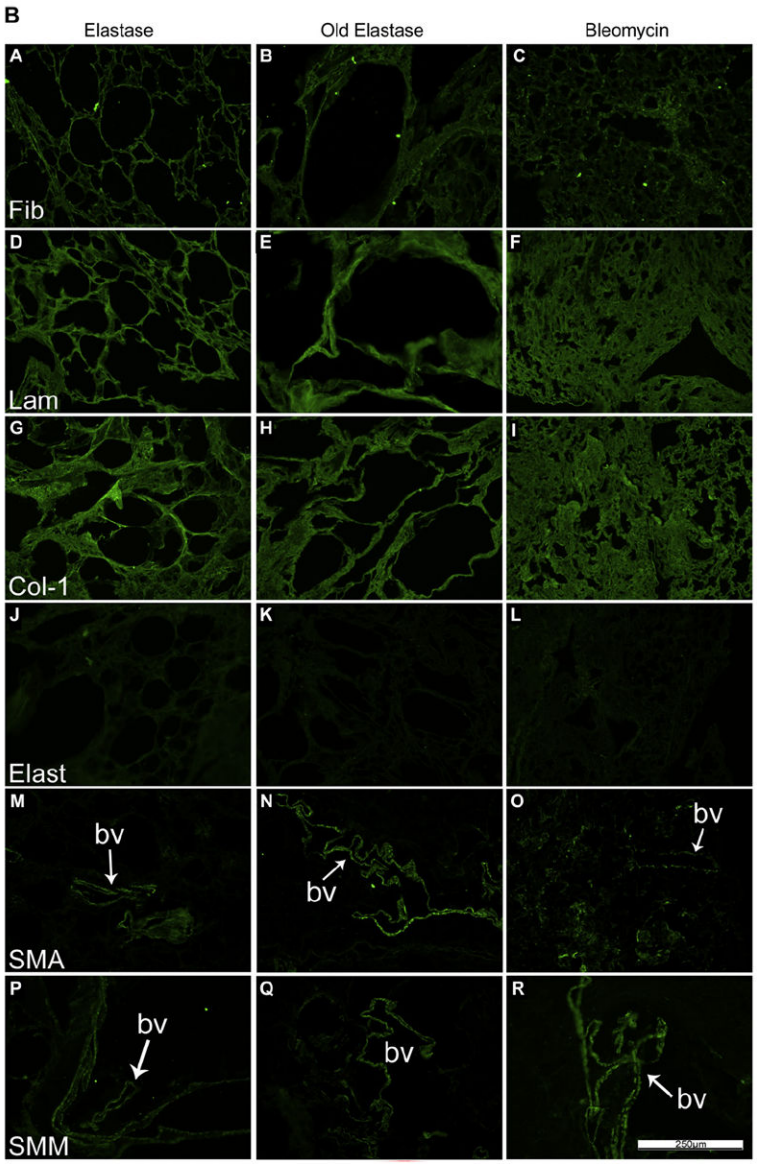

Fig. 2.

A: De-cellularization similarly preserves most ECM proteins in lungs from young vs. old mice. Representative photomicrographs comparing native mouse lung and freshly de-cellularized mouse lungs are depicted. Nuclear DAPI staining is depicted in blue, and the stain(s) of interest are depicted in green in each respective panel. Lam = laminin, Col-1 = type I collagen, Elast = elastin, Fib = fibronectin, SMA = smooth muscle actin, SMM = smooth muscle myosin. a = airways, bv = blood vessels. $N = 6$ for each condition. Original magnification 200×. **B: De-cellularization preserves most ECM proteins in lungs obtained from elastase and bleomycin-treated mice**. Representative photomicrographs are shown. Nuclear DAPI staining is depicted in blue, and the stain(s) of interest are depicted in green in each respective panel. Lam = laminin, Col-1 = type I collagen, Elast = elastin, Fib = fibronectin, SMA = smooth muscle actin, SMM = smooth muscle myosin. a = airspaces, bv = blood vessels. $N = 6$ for each experimental condition. Original magnification 200×.(For

interpretation of the references to colour in this figure legend, the reader is referred to the web version of this article)

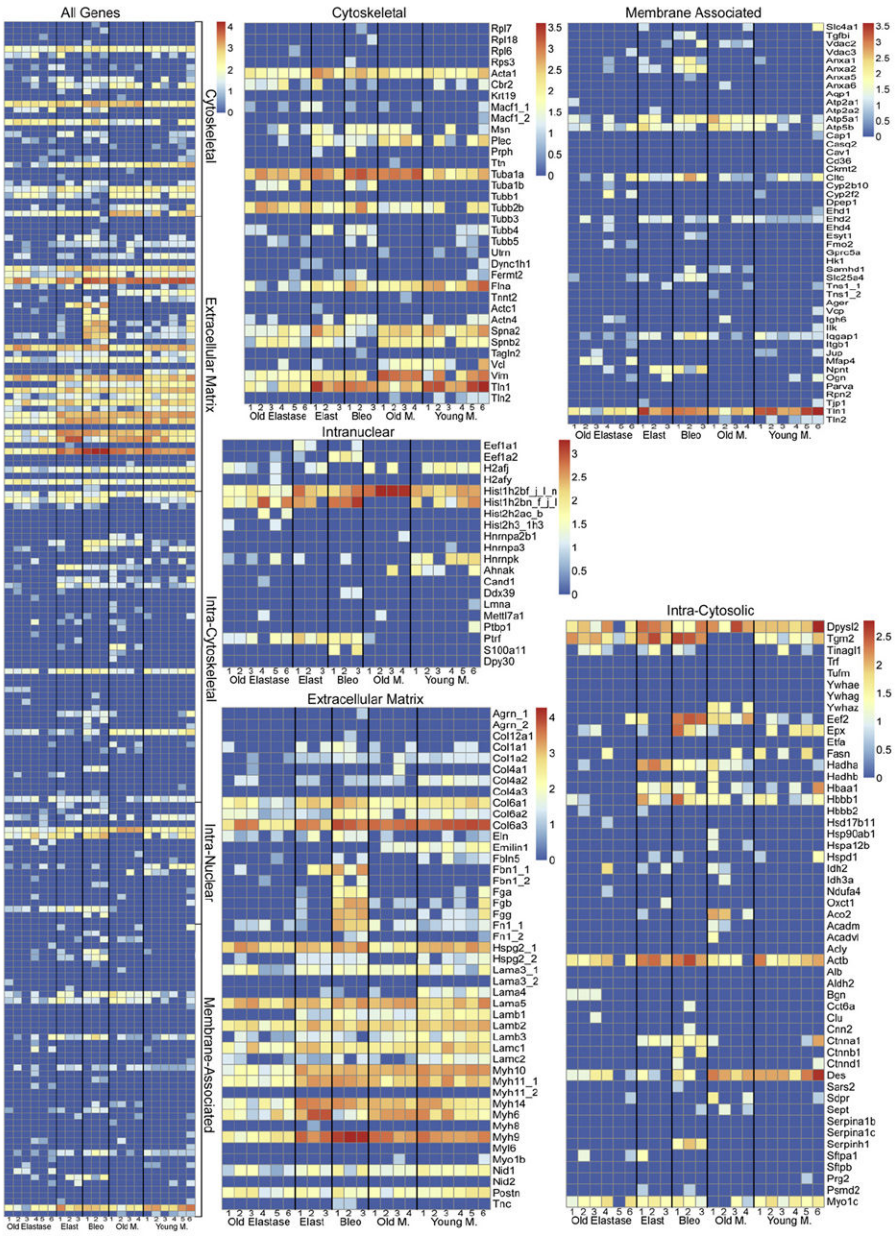

Fig. 3. Heat maps of mass spectrometric assessments of residual proteins

The combined heat map and specific heat maps for each of the designated protein categories are shown. The color scheme represents log order transform values which depict the relative abundance of each protein compared to presence in freshly de-cellularized lungs.

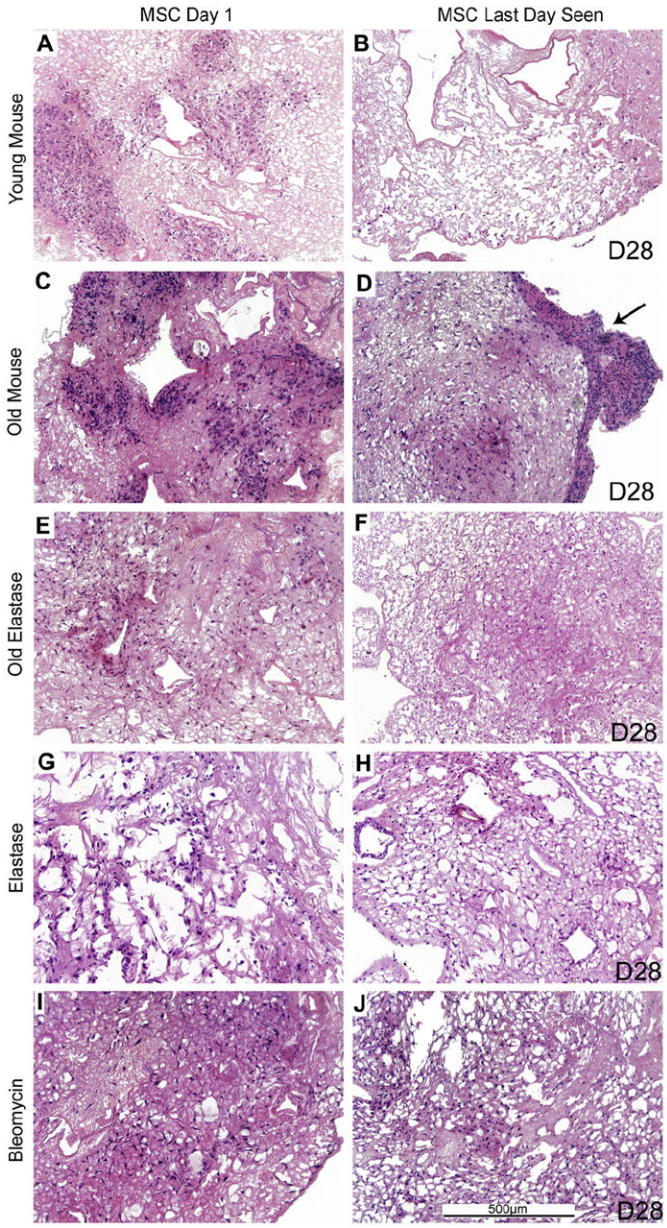

Fig. 4. Growth of MSCs is similar in de-cellularized lungs obtained from aged and injured vs. young healthy mice

Representative H and E images of de-cellularized aged and injured lungs intratracheally inoculated with MSCs are shown. Images demonstrate characteristic re-cellularization 1 day after inoculation for all conditions (left). Robust recellularization was maintained for 28 days in culture (right) for all conditions. The arrow indicates an area where the MSCs migrated out of the de-cellularized lung slices and formed agglomerates on plastic of the tissue culture dish. a = airspaces, bv = blood vessels. $N = 3$ for each experimental condition. Original magnification 100×.

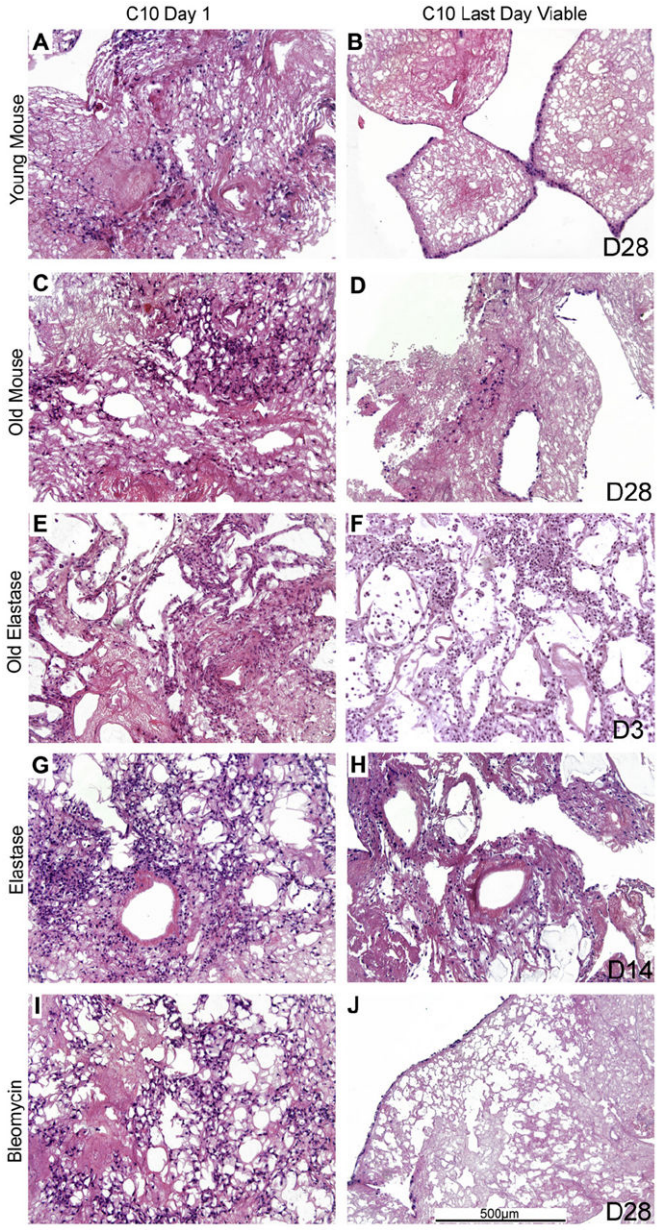

Fig. 5. C10 epithelial cells have decreased long-term survival in de-cellularized lungs obtained from elastase-treated mice

Representative H&E images of various decellularized lungs treated under different storage and sterilization techniques intratracheally inoculated with C10 cells. Images show characteristic re-cellularization 1 day after inoculation (left) in addition to the time point at which the last viable cells were observed (right). The last day cells were observed is indicated on the figure (e.g. D14 is day 14). a = airspaces, bv = blood vessels. $N = 3$ for each experimental condition. Original magnification 100×.

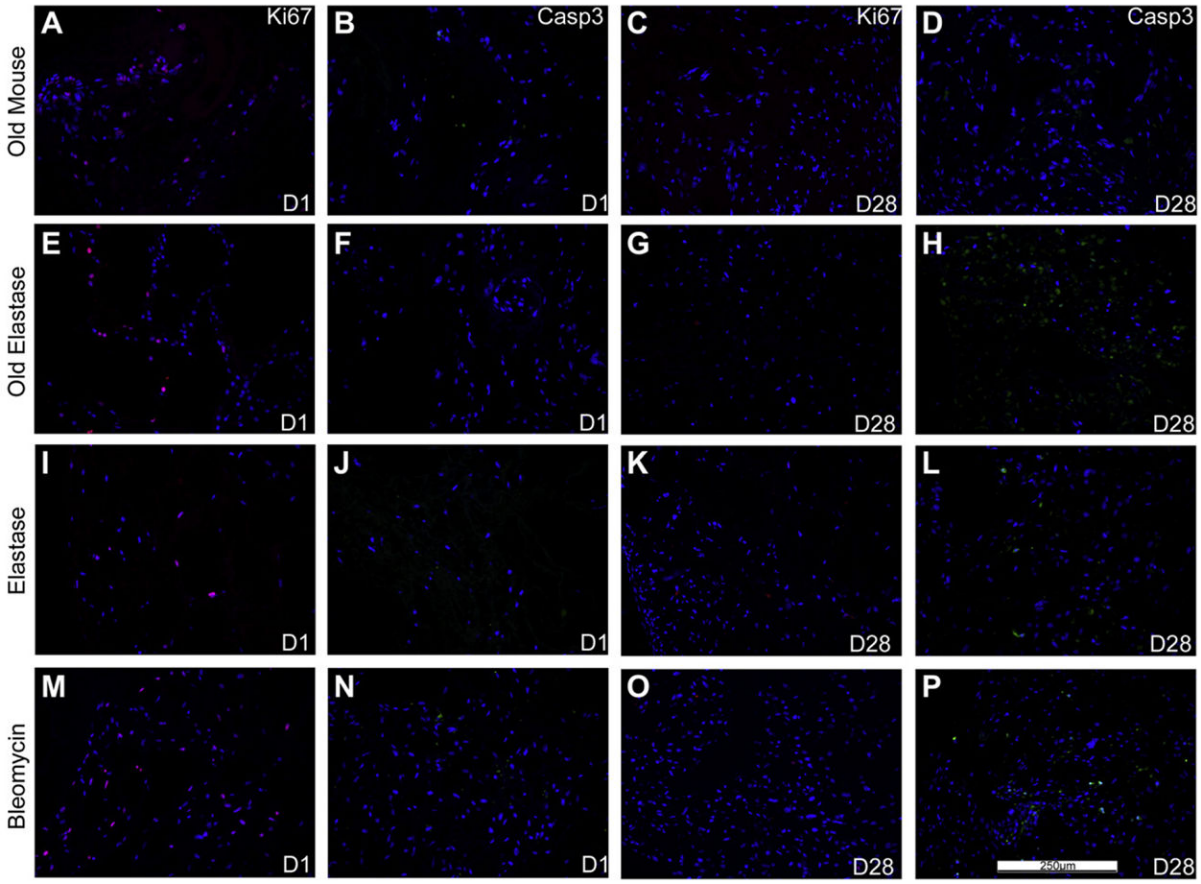

Fig. 6. MSCs inoculated into the de-cellularized lungs demonstrate similar sustained proliferation by Ki67 staining and minimal apoptosis by caspase-3 staining

Representative photomicrographs of characteristic Ki67 (red) or caspase-3 (green) are shown at 1 and 28 days post-inoculation. For both panels, caspase-3 immunofluorescence is depicted in green and Ki67 immunofluorescence is depicted in red. DAPI nuclear staining is depicted in blue. a = airways, bv = blood vessels. $N = 3$ for each experimental condition. Original magnification 200×. (For interpretation of the references to colour in this figure legend, the reader is referred to the web version of this article)

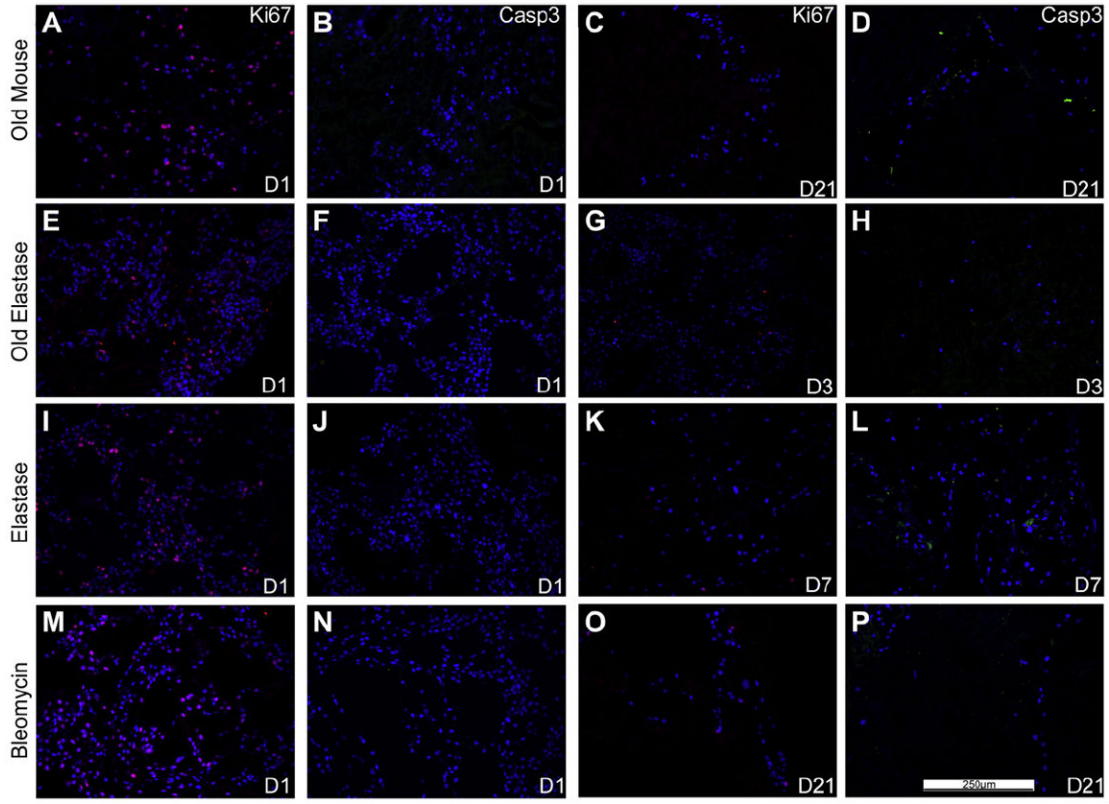

Fig. 7. C10s inoculated into various storage and sterilized de-cellularized lungs demonstrate diminished proliferation by Ki67 staining and increased apoptosis by caspase-3 staining

Representative photomicrographs of characteristic Ki67 (red) or caspase-3 (green) are shown at 1 day post-inoculation (left) as well as at time points in which caspase-3 staining was increased at or prior to the time when viable cells were last observed (e.g. D7 is day 7). For both panels, caspase-3 immunofluorescence is depicted in green and Ki67 immunofluorescence is depicted in red. DAPI nuclear staining is depicted in blue. a = airways, bv = blood vessels. $N = 3$ for each experimental condition. Original magnification 200×.(For interpretation of the references to colour in this figure legend, the reader is referred to the web version of this article)

Biomaterials. Author manuscript; available in PMC 2014 October 31.

Table 1

Statistical analysis of differences in mass spectrometry from de-cellularized aged and emphysematous and fibrotic injured mouse lungs.

Gene	Protein name	vs. RLL				vs. Elast	vs. Oldlg	IPI
		Old lung	Elast	Old elast	Bleo	Old elast	Old elast	
Cytoskeletal								
Actn4	Alpha-actinin-4	0.200	1.000	0.470	***0.048***	0.643	0.467	IPI00118899.1
Cbr2	Carbonyl reductase [NADPH] 2	0.200	0.821	0.320	0.905	0.952	***0.043***	IPI00128642.1
Flna	Isoform 1 of Filamin-A	0.086	0.107	**0.002**	0.310	**0.024**	**0.005**	IPI00131138.10
Plec	Plectin isoform 1b2alpha	0.200	0.833	0.106	0.750	**0.024**	**0.005**	IPI00229509.3
Spna2	Isoform 2 of Spectrin alpha chain, brain	0.810	0.833	**0.011**	**0.036**	**0.012**	**0.014**	IPI00753793.2
Tuba1a	Tubulin alpha-1A chain	***0.005***	0.119	0.087	***0.012***	0.714	**0.010**	IPI00110753.1
Tuba1b	Tubulin alpha-1B chain	1.000	1.000	0.061	***0.012***	0.155	0.133	IPI00117348.4
Tubb2b	Tubulin beta-2B chain	0.910	0.571	***0.022***	0.119	0.071	***0.010***	IPI00109061.1
Vcl	Vinculin	0.952	0.357	0.106	0.214	1.000	**0.010**	IPI00405227.3
Vim	Vimentin	***0.048***	0.714	0.158	0.381	**0.012**	**0.005**	IPI00227299.6
Extracellular matrix proteins								
Col1a2	Collagen alpha-2(I) chain	0.281	**0.048**	**0.002**	1.000	**0.012**	0.067	IPI00222188.4
Col4a2	Collagen alpha-2(IV) chain	**0.019**	**0.012**	**0.013**	**0.012**	0.762	0.524	IPI00338452.3
Col6a1	Collagen alpha-1(VI) chain	**0.005**	0.274	**0.013**	***0.024***	**0.036**	0.381	IPI00339885.2
Col6a2	Collagen alpha-2(VI) chain	0.938	0.155	0.485	***0.036***	0.393	0.829	IPI00621027.2
Col6a3	collagen alpha-3(VI) chain	0.133	**0.024**	**0.004**	0.702	0.238	**0.019**	IPI00830749.3
Eln	Elastin	0.619	0.548	0.632	***0.024***	0.738	0.381	IPI00134505.1
Emilin1	EMILIN-1	0.057	**0.012**	**0.002**	**0.012**	1.000	**0.033**	IPI00115516.1
Fbln5	Fibulin-5	**0.033**	0.083	**0.028**	0.929	1.000	1.000	IPI00323035.3
Fbn1_1	Fibrillin-1	1.000	0.083	1.000	***0.012***	0.083	1.000	IPI00122438.1
Fga	Fibrinogen, alpha polypeptide isoform 2	0.467	0.750	0.455	***0.012***	0.333	1.000	IPI00115522.3
Fgb	Fibrinogen beta chain	0.957	0.810	0.182	***0.012***	0.333	**0.033**	IPI00279079.1
Fgg	Putative uncharacterized protein	**0.043**	0.202	**0.015**	***0.012***	0.333	1.000	IPI00122312.2
Fn1_1	Fibronectin	0.871	**0.024**	0.303	***0.012***	0.202	0.400	IPI00113539.2
Hspg2_1	Basement membrane-specific heparan sulfate proteoglycan core protein	**0.005**	0.333	0.275	0.262	1.000	***0.043***	IPI00113824.1
Hspg2_2	Basement membrane-specific heparan sulfate proteoglycan core protein	**0.033**	1.000	**0.028**	0.881	**0.012**	1.000	IPI00515360.8

Gene	Protein name	vs. RLL				vs. Elast	vs. Oldlg	IPI
		Old lung	Elast	Old elast	Bleo	Old elast	Old elast	
Lama4	Laminin subunit alpha-4	**0.014**	**0.036**	**0.002**	**0.024**	0.333	0.400	IPI00223446.5
Lama5	Laminin subunit alpha-5	0.329	0.643	0.693	0.321	0.917	0.200	IPI00116913.3
Lamb1	Laminin subunit beta-1	**0.010**	**0.012**	**0.002**	0.060	**0.012**	**0.005**	IPI00338785.3
Lamb2	Laminin subunit beta-2 precursor	**0.029**	0.393	**0.004**	0.321	0.119	0.114	IPI00109612.2
Lamb3	Laminin subunit beta-3	0.243	0.214	**0.006**	0.060	0.071	**0.048**	IPI00117093.1
Lamc1	Laminin subunit gamma-1	0.143	0.893	**0.045**	0.333	0.071	0.310	IPI00400016.1
Lamc2	Laminin subunit gamma-2	**0.005**	**0.012**	**0.004**	0.155	0.488	0.857	IPI00117115.3
Myh10	Myosin, heavy polypeptide 10, non-muscle	**0.038**	0.107	**0.002**	**0.048**	**0.012**	**0.005**	IPI00338604.5
Myh11_1	Isoform 1 of Myosin-11	0.357	0.571	**0.002**	0.298	**0.012**	**0.014**	IPI00114894.1
Myh14	Isoform 1 of Myosin-14	0.567	0.060	**0.004**	0.167	**0.012**	**0.005**	IPI00453996.1
Myh6	Myosin-6	0.162	***0.048***	0.095	0.095	**0.012**	**0.005**	IPI00129404.1
Myh9	Myosin-9	0.562	0.155	**0.002**	***0.012***	**0.012**	**0.005**	IPI00123181.4
Nid1	Nidogen-1	**0.019**	0.167	**0.022**	1.000	0.345	0.467	IPI00111793.1
Intracellular cytoplasmic								
Aco2	Aconitate hydratase, mitochondrial	***0.033***	0.333	1.000	1.000	0.333	**0.033**	IPI00116074.1
Actb	Actin, cytoplasmic 1	0.076	0.155	0.227	0.071	**0.024**	0.500	IPI00110850.1
Ctnna1	Catenin alpha-1	0.900	0.536	0.455	0.202	**0.012**	0.400	IPI00112963.1
Des	Desmin	0.729	**0.012**	**0.006**	0.060	0.583	**0.010**	IPI00130102.4
Dpysl2	Dihydropyrimidinase-related protein 2	1.000	0.631	0.132	0.512	**0.048**	0.152	IPI00114375.2
Eef2	Elongation factor 2	***0.010***	0.940	0.697	***0.012***	0.750	**0.010**	IPI00466069.3
Hadha	Trifunctional enzyme subunit alpha, mitochondrial	***0.010***	***0.012***	1.000	***0.012***	**0.012**	**0.010**	IPI00223092.5
Hadhb	Trifunctional enzyme subunit beta, mitochondrial	0.400	1.000	1.000	1.000	1.000	0.400	IPI00115607.3
Hbaa1	Putative uncharacterized protein	1.000	0.440	0.182	1.000	**0.012**	**0.033**	IPI00110658.1
Hbbb1	LOC100503164 Beta-globin	0.867	0.393	0.069	0.095	**0.036**	0.095	IPI00762198.2
Myo1c	Isoform 2 of Myosin-Ic	**0.019**	1.000	0.673	0.750	0.893	0.143	IPI00467172.2
Serpinh1	Serpin H1	1.000	1.000	1.000	***0.012***	1.000	1.000	IPI00114733.1
Tgm2	Protein-glutamine gamma-glutamyltransferase 2	**0.005**	***0.024***	0.141	***0.012***	0.202	***0.010***	IPI00126861.3
Ywhaz	14-3-3 protein zeta/delta	***0.033***	1.000	1.000	1.000	1.000	**0.033**	IPI00116498.1
Intracellular nuclear								
Eef1a2	Elongation factor 1-alpha 2	1.000	0.333	1.000	***0.012***	1.000	1.000	IPI00119667.1

Gene	Protein name	vs. RLL				vs. Elast	vs. Oldlg	IPI
		Old lung	Elast	Old elast	Bleo	Old elast	Old elast	
Hist1h2bf_j_l_n	Histone H4	***0.005***	0.631	**0.004**	0.607	**0.012**	**0.005**	IPI00407339.7
Hist1h2bn_f_j_l	Histone Type 1-F/J/L.	**0.033**	0.893	0.552	***0.024***	0.798	***0.019***	IPI00114642.4
Hnrnpk	Isoform 2 of Heterogeneous nuclear ribonucleoprotein K	**0.033**	0.083	**0.035**	0.083	0.821	0.200	IPI00224575.1
Ptrf	Polymerase I and transcript release factor	0.400	***0.012***	***0.015***	***0.012***	**0.048**	***0.048***	IPI00117689.1
Membrane								
Anxa1	Annexin A1	1.000	0.750	1.000	***0.024***	0.750	1.000	IPI00230395.5
Anxa2	Annexin A2	1.000	0.083	1.000	***0.012***	0.083	1.000	IPI00468203.3
Atp5a1	ATP synthase subunit alpha, mitochondrial	***0.029***	0.714	0.232	***0.048***	0.250	**0.005**	IPI00130280.1
Atp5b	ATP synthase subunit beta, mitochondrial	***0.038***	0.071	0.429	0.857	0.143	0.071	IPI00468481.2
Ehd2	Eh domain-containing protein 1	0.490	***0.036***	0.251	0.488	0.131	0.190	IPI00126083.3
Iqgap1	Ras GTPase-activating-like protein IQGAP1	0.052	0.833	**0.009**	***0.024***	0.202	0.714	IPI00467447.3
Npnt	Isoform 4 of Nephronectin	1.000	0.083	1.000	***0.012***	0.083	1.000	IPI00124689.1
Samhd1	Mimecan	***0.033***	1.000	1.000	0.333	1.000	**0.033**	IPI00120848.1
Slc25a4	ADP/ATP translocase 1	1.000	0.333	0.455	***0.012***	0.643	0.467	IPI00115564.5
Vdac2	Voltage-dependent anion-selective channel protein 2	***0.033***	0.333	1.000	0.333	0.333	**0.033**	IPI00122547.1
Tln1	Talin-1	**0.010**	0.619	**0.002**	0.345	**0.012**	0.129	IPI00465786.3

Values represent *p*-values from two group comparisons of raw unique peptide hits using the non-parametric test (pre-planned, selected, pairwise comparisons are shown in the top two rows). Protein group assignments were generated from UniProt entries of positively identified proteins (proteins containing two or more unique peptide hits). Grayed boxes with italicized text indicate the treatment group (labeled in the second row) reached statistical significance (*p*-values less than 0.05) with higher amounts of unique peptide hits than the control group. White boxes with black bolded text indicate the control group (labeled in the top row) contained significantly more unique peptide hits.

Italics – treatment group significantly higher.

Black – control significantly higher (designated above).

Key: Elas = Elastase; Bleo = Bleomycin; Old Elast = Old Elastase; Oldlg = Old Mouse; RLL = Young Mouse, Right Lower Lobe.